Journal of Physiology (1996), **491.1**, *pp.*137–150

Effects of intracellular Mg^{2+} on channel gating and steady-state responses of the NMDA receptor in cultured rat neurons

Yingying Li-Smerin and Jon W. Johnson

Department of Neuroscience, University of Pittsburgh, Pittsburgh, PA 15260, USA

1. The effects of intracellular Mg^{2+} (Mg_i^{2+}) on the single *N*-methyl-D-aspartate (NMDA)-activated channel burst duration and frequency and on the mean NMDA-activated patch current were studied in outside-out patches from cultured rat cortical neurons. The inhibition by Mg_i^{2+} of mean patch and whole-cell currents were compared, and some possible explanations for the observed differences were investigated.

2. The burst duration at +60 mV did not depend on Mg_i^{2+} concentration, suggesting that the channel can close when blocked by Mg_i^{2+}. The number of bursts per second increased significantly in the presence of Mg_i^{2+}, suggesting that the rate of channel opening is higher when Mg^{2+} from the intracellular solution occupies its binding site.

3. Mg_i^{2+} caused a voltage- and concentration-dependent inhibition of mean patch current. The inhibition is in quantitative agreement with the effects of Mg_i^{2+} on the single-channel current and on burst parameters.

4. Based on the effects of Mg_i^{2+} on burst parameters and on single-channel current, a four-state model in which the NMDA-activated channel can close while blocked by Mg_i^{2+} is proposed. By fitting the model to the mean patch current data, we estimate that the rate of channel opening is increased by a factor of 1·4 when Mg_i^{2+} occupies the channel. This estimation provides evidence that occupancy of the NMDA-activated channel by Mg_i^{2+} destabilizes the closed state.

5. Mg_i^{2+} reduced NMDA-activated whole-cell currents in a voltage- and concentration-dependent manner. However, normalized whole-cell and mean patch currents at positive voltages differed in two significant respects. First, when currents were recorded in a 0 Mg^{2+} pipette solution, whole-cell currents at positive voltages were smaller. Second, Mg_i^{2+} appeared to inhibit whole-cell current less effectively than it inhibited mean patch current.

6. Inclusion of the Mg^{2+} chelators EDTA and ATP in 0 Mg^{2+} pipette solutions did not increase the whole-cell current measured at +60 mV. This observation suggests that the difference between normalized whole-cell and mean patch currents with 0 Mg^{2+} pipette solution was not due to block of whole-cell currents by residual Mg_i^{2+}.

7. When a pipette solution containing EGTA and Mg^{2+} was used to buffer Mg_i^{2+}, inhibition by Mg_i^{2+} of the whole-cell current was enhanced, suggesting that the free Mg^{2+} concentration inside a neuron can remain below the pipette Mg^{2+} concentration. However, we cannot exclude other explanations for the differences between the inhibition by Mg^{2+} of mean patch and whole-cell currents.

In the preceding paper (Li-Smerin & Johnson, 1996), we examined the kinetics with which intracellular Mg^{2+} (Mg_i^{2+}) blocks current flow through single *N*-methyl-D-aspartate (NMDA)-activated channels. The voltage and concentration dependence of the kinetics of Mg_i^{2+} block was shown to be consistent with a simple two-state model of the interaction of Mg_i^{2+} with the open NMDA-activated channel. However, neither the kinetic data nor the model addressed the question of how channel block by Mg_i^{2+} affects channel gating. Quantification of the effects of Mg_i^{2+} block on channel gating is required to predict how Mg_i^{2+} should influence NMDA receptor-dependent processes such as synaptic transmission and glutamate-induced cell death. If the channel cannot close while blocked by Mg_i^{2+}, for example, then Mg_i^{2+} will cause less inhibition of NMDA receptor-dependent current flow than if Mg_i^{2+} permits

channel closure. This prediction results from the increase in single-channel burst duration that is observed in the presence of channel blockers that prevent channel closure (Neher & Steinbach, 1978). Block of the NMDA-activated channel by extracellular Mg^{2+} (Mg_o^{2+}) does not cause an increase in single-channel burst duration (Ascher & Nowak, 1988). Based in part on analysis of bursts, Jahr & Stevens (1990) proposed a four-state model of channel block by Mg_o^{2+} in which the channel of the NMDA receptor could close while blocked. Our first goal in this study was to refine our model of block by Mg_i^{2+} by determining the effects of Mg_i^{2+} on NMDA-activated channel gating.

To test the validity and generality of predictions made from single-channel analysis, we investigated the effects of Mg_i^{2+} on steady-state NMDA-activated currents from patch and whole-cell preparations. We first examined the inhibition by Mg_i^{2+} of the mean current flow through outside-out patches during prolonged applications of NMDA. We used outside-out patches for these measurements to take advantage of the excellent control of membrane voltage and concentration of intracellular constituents possible with this approach. In addition, measurements of mean patch current allowed us to estimate the net inhibition due to Mg_i^{2+} more accurately and over a wider range of conditions than was possible with single-channel recording. The results were consistent with our single-channel measurements, and allowed us to quantify the effect of block by Mg_i^{2+} on channel gating. To compare predictions based on patch experiments with results from a more intact preparation, we also examined the effect of Mg_i^{2+} on the whole-cell current. While whole-cell currents were also inhibited, Mg_i^{2+} appeared to be less effective than in patches. The results of further whole-cell experiments suggested that the free Mg^{2+} concentration in the pipette and within the clamped neuron may differ. However, we cannot at present exclude other possibilities, such as a difference between the behaviour of NMDA receptors in the patch and the whole-cell configurations.

Preliminary reports of some of these results have appeared previously (Li & Johnson, 1992; Li-Smerin & Johnson, 1994)

METHODS

Cell culture

All procedures using animals were in accordance with the NIH *Guide for the Care and Use of Laboratory Animals*, and were approved by the University of Pittsburgh's Institutional Animal Care and Use Committee. Primary neuronal cultures were prepared using the methods described by Li-Smerin & Johnson (1996). Briefly, 16 day pregnant rats (Sprague–Dawley), were killed by CO_2 inhalation. Death was confirmed by the absence of a heartbeat. Eight to ten fetuses were removed and chilled to about 5 °C, a scalpel cut through the head that transected the brainstem was made, the brain was removed and the cerebral cortices were isolated. Cortical cells were dissociated and plated onto 15 mm diameter glass coverslips in 35 mm plastic Petri dishes. Neurons were used after 7–35 days in culture.

Composition of solutions

Unless otherwise indicated, the control (0 Mg_i^{2+}) intracellular solution contained (mM): 125 CsCl, 10 Hepes and 10 EGTA. The pH was adjusted to 7·2 with CsOH. In some whole-cell experiments, the control intracellular solution contained 140 mM CsCl and 10 mM Hepes only. To chelate free Mg_i^{2+}, 10 mM EDTA alone or 10 mM EDTA plus 5 mM Na_2-ATP (Vandenberg, 1987; Sands & Barish, 1992) were added to this 0 EGTA solution. 1 M $MgCl_2$ was diluted into the control intracellular solution, with or without EGTA, to give the indicated final free Mg^{2+} concentration. The free Mg^{2+} concentration was corrected for Mg^{2+} bound to EGTA as described by Li-Smerin & Johnson (1996). The control extracellular solution contained (mM): 140 NaCl, 2·8 KCl, 1 $CaCl_2$, 10 Hepes and 0·0002 TTX. The pH was adjusted to 7·2 with NaOH. The solution used to activate the NMDA receptor (NMDA solution) contained 30 μM NMDA plus 10 μM glycine. All chemicals were purchased from Sigma or Aldrich.

Recording Conditions

The outside-out patch recordings used for single-channel analysis by Li-Smerin & Johnson (1996) were also used for burst analysis and mean patch current measurements here. Whole-cell recordings were performed using conventional patch-clamp techniques (Hamill, Marty, Neher, Sakmann & Sigworth, 1981). Pipettes were pulled from either soft glass (KG-12) capillaries or borosilicate thin-wall glass capillaries with inner filaments (Clark Electromedical Instruments, Reading, UK). The pipette resistance was 1–5 MΩ. Compensation for series resistance was not performed. Neurons used for whole-cell recordings were typically 15–30 μm in diameter. Whole-cell recordings were discarded if the absolute current at any voltage was larger than 2 nA. In about 25% of our experiments, the maximal amplitude of the whole-cell current exceeded 1 nA. The series resistance error during maximal current flow for these cells ($n = 10$), assuming that the series resistance was twice the pipette resistance, was 4·1–12·8 mV (see Discussion). Data from any cell with a voltage drift larger than 4 mV were discarded. Solutions were applied as described by Li-Smerin & Johnson (1996).

During whole-cell experiments, the baseline current and the NMDA response at each test voltage were recorded by alternately superfusing the neuron with the corresponding solutions. Each application of NMDA solution, which typically lasted 20–40 s, was preceded and followed by applications of the control solution. The whole-cell responses were recorded at membrane potentials ranging from −60 to +60 mV in the following order: −60, +60, −40, +40, −20 and +20 mV. To ensure that a steady state was reached after each change in membrane potential, we usually allowed a period of 5–15 s between changing membrane potential and applying the NMDA solution. The first NMDA response was usually recorded about 5 min after breaking the patch to initiate whole-cell recording. We observed that the inhibition by Mg_i^{2+} of the NMDA responses measured early and later (>30 min) in the same neurons was not significantly different (see Results), suggesting that the Mg^{2+} concentration inside the neuron reached steady-state levels within 5 min. This estimation is consistent with other reports (Pusch & Neher, 1988; Zarei & Dani, 1995). Measurement of the whole-cell current at −60 mV was repeated periodically during each experiment to monitor the stationarity of the NMDA response magnitude. Any cell in which the current at

−60 mV varied during an experiment by more than 25% from the first measurement was discarded.

Data analysis

Analysis of bursts. The details of data filtering, sampling for off-line analysis and the acquisition and editing of single-channel data were described by Li-Smerin & Johnson (1996). The mean open time, the frequency of openings and the closed time distributions were analysed using both the Channel Analysis Program (RC Electronics, Goleta, CA, USA) and a program written using the AxoBASIC programming environment (Axon Instruments). Individual openings and closures of single channels were detected using a 50%-threshold-crossing criterion. Burst duration and burst frequency were analysed after eliminating brief events (see Results). The mean burst duration was obtained by fitting unbinned data using the maximum likelihood method (Colquhoun & Sigworth, 1983). When brief events were eliminated from dwell time histograms, the duration ignored was subtracted from the mean dwell times estimated by maximum likelihood (Colquhoun & Sigworth, 1983).

Measurements of mean patch current. Patch current was recorded for at least 1 min at each membrane potential. Generally, two to four such segments were recorded at −40, −20, +20, +40 or +60 mV, separated by segments at −60 mV. Amplitude histograms constructed using all sampled points (see Fig. 2) were used to calculate total charge flow through open channels (including multilevel openings) during each segment. Bins below 50% of the first open-channel current level were not included in the calculation. Mean patch current was calculated by dividing total charge flow by the duration of the analysed segment. The construction of amplitude histograms and the determination of mean patch current were performed with programs written using the AxoBASIC programming environment. Whenever the mean patch current values of two segments measured at −60 mV, which preceded and followed a segment measured at a different voltage, varied from each other by more than 30%, the data between the two segments were discarded.

To calculate the average value of mean patch current from several patches, each mean patch current was weighted by the total charge measured in that patch at positive potentials. We chose this way of weighting the averages because patches with greater charge flow due to higher activity and/or longer recording times should provide more accurate estimates of mean current. The standard error of the weighted mean was estimated according to the procedure described in Cochran (1956).

Measurements of whole-cell current. The amplitude of the steady-state whole-cell current was calculated by subtracting the holding current measured in control solution from the current measured in NMDA solution. Cells were discarded if the baseline current before and after any single application of the NMDA solution changed by more than 25% of the NMDA response measured at −60 mV in the same neuron.

To allow comparisons between cells and/or patches, we normalized the whole-cell and the mean patch currents to those measured at −60 mV, a voltage at which the Mg_i^{2+} block is minimal. The current–voltage (I_p–V) plots of mean patch current (see Fig. 3) were fitted with equations described in Results using the Marquardt–Levenberg algorithm in SigmaPlot 5.0. Results are presented as means ± S.E.M. Statistical comparisons were performed with Systat. The significance level was set at $P < 0.05$.

RESULTS

Effects of Mg_i^{2+} on the burst duration and frequency

To investigate how Mg_i^{2+} binding affects channel gating and to refine the model of block proposed previously (Johnson & Ascher, 1990; Li-Smerin & Johnson, 1996), we analysed the effects of Mg_i^{2+} on bursts of openings. Analysis of bursts was limited to recordings at +60 mV with 0, 1 or 3 mM Mg_i^{2+} because with 10 mM Mg_i^{2+} or at less positive voltages the small apparent single-channel current amplitude and large noise caused by Mg_i^{2+} block precluded accurate analysis.

The idealized burst in the presence of Mg_i^{2+} that we wished to identify consists of channel alterations between the open–unblocked and open–blocked states during a channel opening (e.g. see Neher & Steinbach, 1978). Because of the rapid unbinding rate of Mg_i^{2+}, the apparent open time in the presence of Mg_i^{2+} should in principle equal the desired burst duration, and use of the critical time (t_{crit}) should not be required. However, analysis of bursts was complicated by the decrease in apparent single-channel current amplitude and increase in apparent open-channel noise caused by Mg_i^{2+}. Both these effects cause increasing numbers of artifactual closures due to crossings of the half-amplitude threshold as the Mg_i^{2+} concentration is increased (see, e.g. Fig. 2*A* in Li-Smerin & Johnson, 1996). We minimized the errors due to noise-induced threshold crossings by ignoring closures of equal to or less than a specified critical closed time ($t_{crit,c}$), with $t_{crit,c}$ chosen such that it was longer than the vast majority of artifactual closures. The value of $t_{crit,c}$ was determined empirically by measuring the burst frequency and duration with 3 mM Mg_i^{2+} at +60 mV as a function of $t_{crit,c}$. As $t_{crit,c}$ was increased from 0·2 ms, the burst frequency decreased and the burst duration initially increased steeply, but approached a plateau value by 1 ms. Because of the presence of relatively frequent double openings, we could not rely on the closed time distribution to accurately select $t_{crit,c}$. Nevertheless, our analysis of closed time distributions, and visual inspection of single-channel records, support the validity of the selection of a value of $t_{crit,c}$ of 1 ms.

The value of $t_{crit,c}$ used in this study is similar to the value used by Gibb & Colquhoun (1992) to define bursts of NMDA-activated channel openings (mean value, 1·85 ms). Because we observed that burst frequency and duration were not very sensitive to variations of $t_{crit,c}$ from 0·8 to 2 ms, it is likely that the control bursts as defined here correspond approximately to the bursts defined by Gibb & Colquhoun (1992). However, it should be kept in mind that the goal of the burst analysis in their study was quite different from our goal to eliminate artifacts due to noise-induced threshold crossings.

The decrease in the apparent single-channel current caused by Mg_i^{2+} and the resulting decrease in half-amplitude threshold also caused an increase in the number of baseline noise excursions that were artifactually counted as openings. We reduced this error by ignoring openings of less than or equal to a specified critical open time ($t_{crit,o}$), with $t_{crit,o}$ chosen such that it was longer than the vast majority of artifactual openings. To choose $t_{crit,o}$, sections of current records at +60 mV with 3 mM Mg_i^{2+} that lacked channel openings were selected, the threshold was set at 50% of the first open-channel current level measured in the same patch, and the frequency of artifactual openings was measured. The apparent frequency of opening decreased abruptly as $t_{crit,o}$ was increased from 0 to 0·4 ms, and approached zero at 0·4 ms. Setting $t_{crit,o}$ equal to 0·4 ms therefore should eliminate the vast majority of threshold crossings due to baseline noise, while minimizing the number of real openings that are excluded. The exclusion of such brief openings would significantly influence our conclusions only if the Mg_i^{2+} actions depended on channel open duration, which seems unlikely. Based on these results, closures of $\leqslant$ 1 ms and then openings of $\leqslant$ 0·4 ms were eliminated from burst analysis. This procedure reduced the number of openings at +60 mV by 39% at 0 mM Mg_i^{2+}, by 72% with 1 mM Mg_i^{2+}, and by 80% with 3 mM Mg_i^{2+}.

Under control conditions the frequency and duration of bursts of the NMDA-activated channel were voltage dependent. The burst frequency was 54% greater and the burst duration 28% greater at +60 than at −60 mV. The voltage sensitivity of the burst frequency and duration of NMDA-activated channels are qualitatively consistent with the results of Nowak & Wright (1992).

The effect of Mg_i^{2+} on burst frequency is presented in Fig. 1*A*. To permit pooling of data from different patches, the burst frequency measured at +60 mV was normalized to that measured at −60 mV from the same patch. The normalized burst frequency was 1·5 ± 0·1, 2·0 ± 0·3 and 2·5 ± 0·3 at 0, 1 and 3 mM Mg_i^{2+}, respectively. In agreement with these data, analysis of closed time distributions revealed a Mg_i^{2+}-dependent decrease in the closed time between bursts (data not shown). The increase in the burst frequency was associated with a non-significant decrease in burst duration from 11·4 ± 1·2 ms at 0 mM Mg_i^{2+} to 11·1 ± 0·9 ms with 1 mM Mg_i^{2+} and 10·3 ± 0·6 ms with 3 mM Mg_i^{2+} (Fig. 1*B*). The lack of an increase in the burst duration strongly suggests that the channel can close with Mg_i^{2+} blocking it.

Effect of Mg_i^{2+} on the mean patch current

Since Mg_i^{2+} affects channel gating while blocking current flow, measurement of the reduction in the apparent amplitude of single-channel current cannot be expected to reflect the full effect of Mg_i^{2+} on steady-state NMDA-activated currents. Our next goal was to measure accurately the inhibition by Mg_i^{2+} of steady-state current under the conditions in which we had maximal control of the composition of the intracellular solution and of

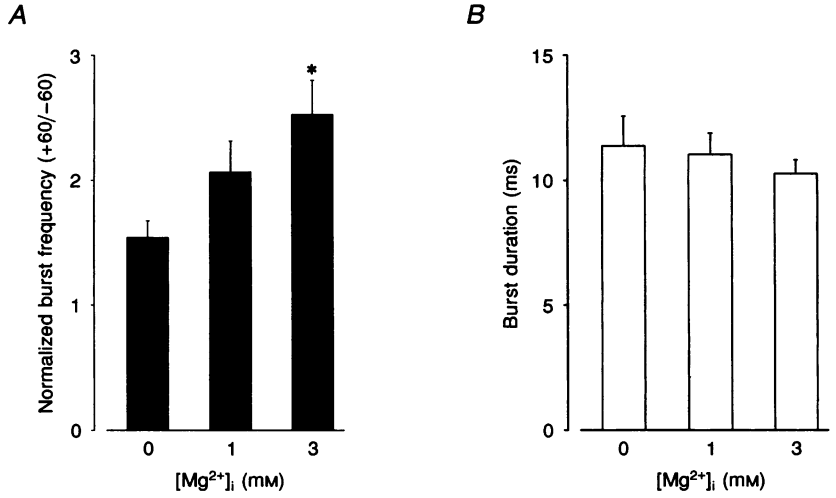

Figure 1. Effects of Mg_i^{2+} on burst frequency and burst duration

A, burst frequency at +60 mV was normalized to that measured at −60 mV from the same patch. In the absence of Mg_i^{2+} ($n = 3$) burst frequency was higher at +60 mV than at −60 mV. In the presence of 1 mM ($n = 3$) and 3 mM ($n = 3$) Mg_i^{2+}, normalized burst frequency was increased. The difference between 0 and 3 mM was significant (* $P < 0·05$; ANOVA followed by Tukey's honestly significant difference (HSD) test). *B*, burst duration at +60 mV was measured from the same patch recordings as used for *A*. The burst duration appeared to decrease as Mg_i^{2+} concentration increased, but the effect of Mg_i^{2+} was not significant (ANOVA).

membrane voltage. We approached this goal by measuring the mean NMDA-activated current flow of outside-out patches.

Measurements of mean patch current in the absence and presence of Mg_i^{2+}

Examples of the all-point histograms used to measure mean patch current are shown in Fig. 2. In 0 mM Mg_i^{2+}, the amplitudes of the single-channel current were equal at −60 and +60 mV. The mean patch current, however, was larger at +60 than at −60 mV due to a higher open probability at +60 mV. Because the pair of histograms at each Mg_i^{2+} concentration were from recordings of similar duration in the same patch, the increase in open probability at +60 mV in 0 mM Mg_i^{2+} is reflected by the increased area of the open-channel peaks. In the presence of 3 mM Mg_i^{2+}, the amplitude of the single-channel current was much smaller at +60 than at −60 mV. As a result, the mean patch current was smaller at +60 than at −60 mV, despite the greater open probability at +60 mV.

Figure 3 presents the $I_p - V$ relationship of the mean patch current measured in the absence and presence of Mg_i^{2+}. The control mean patch current showed a striking outward rectification, in contrast to the nearly linear relationship between the single-channel current amplitude and voltage in the same patches (see Fig. 2 in Li-Smerin & Johnson, 1996). This non-linear mean patch $I_p - V$ relationship was due to the increase in open probability at +60 mV relative to −60 mV shown in Fig. 2 (see also Nowak & Wright, 1992).

Mg_i^{2+} reduced the mean patch current in a concentration- and voltage-dependent manner, similar to the reduction in the apparent amplitude of the single-channel current. However, the fractional inhibition was smaller for mean patch current than for apparent single-channel current

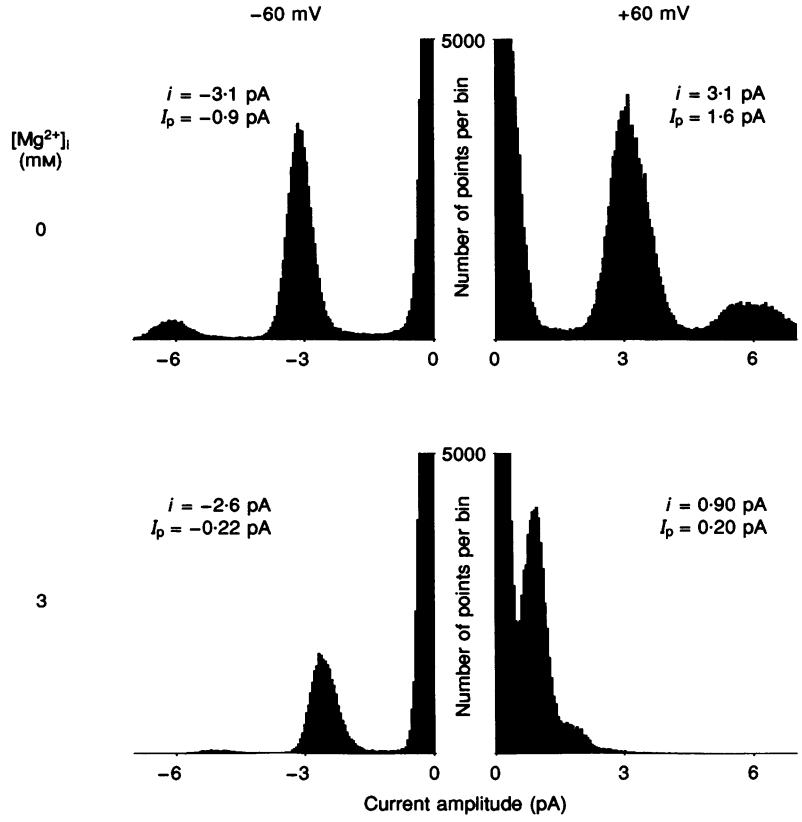

Figure 2. Examples of all-point amplitude histograms measured from outside-out patches in 0 mM (upper panel) and 3 mM (lower panel) Mg_i^{2+} at −60 mV (left) and +60 mV (right)

The bin width is 0·05 pA in all four histograms. At each concentration of Mg_i^{2+} and at each voltage, the amplitude of the baseline current peak was defined as 0 pA; in these figures the baseline peak is truncated. At each concentration of Mg_i^{2+}, the histograms at −60 and +60 mV were from the same patch. i, single-channel current; I_p, mean patch current. The values of NP_o (product of the number of channels in the patch and the channel open probability), calculated by dividing the mean patch current by the single-channel amplitude, were: 0·29 (0 mM Mg_i^{2+}, −60 mV); 0·52 (0 mM Mg_i^{2+}, +60 mV); 0·08 (3 mM Mg_i^{2+}, −60 mV); and 0·22 (3 mM Mg_i^{2+}, +60 mV). The duration of the recordings were: 49 s (0 mM Mg_i^{2+}, −60 mV); 55 s (0 mM Mg_i^{2+}, +60 mV); and 61 s (3 mM Mg_i^{2+}, −60 and +60 mV).

amplitude (Fig. 3, inset). We next tested whether this discrepancy could be explained by the results of burst analysis.

Comparison of measured and predicted mean patch currents

Mean patch current depends on channel open probability as well as single-channel current. The observed effect of Mg_i^{2+} on burst parameters (Fig. 1) therefore should fully explain the discrepancy between inhibition by Mg_i^{2+} of mean patch and of apparent single-channel currents if our burst analysis was accurate. To test this hypothesis, we predicted the normalized patch current ($I_{p,n}$) at +60 mV in the presence of 0, 1 and 3 mM Mg_i^{2+} with the following equation:

$$I_{p,n} = f_b \tau_b i, \quad (1)$$

where f_b is the normalized burst frequency, τ_b is the normalized mean burst duration, and i the normalized apparent amplitude of single-channel current. Because of the fast kinetics of block by Mg_i^{2+}, i represents the product of the unblocked single-channel current amplitude and the probability of a channel being open within bursts. Normalization of all parameters to the values measured at −60 mV allowed elimination from our calculations of the number of channels in the patch.

As shown in Fig. 4*A*, Mg_i^{2+} reduced i, but increased $f_b\tau_b$. The mean patch currents predicted from single-channel parameters (eqn (1)) is in good agreement with mean patch current measured directly (Fig. 4*B*), supporting the hypothesis that the effects of Mg_i^{2+} on both single-channel current and on channel gating can account for the inhibition by Mg_i^{2+} of mean patch current. Furthermore, although the comparison was possible under a limited range of conditions, the close agreement supports the validity of the burst analysis.

Model of the interaction of Mg_i^{2+} with the NMDA-activated channel

The lack of an increase in the burst duration conflicts with the prediction of models in which the open–blocked channel cannot close (Neher & Steinbach, 1978), and suggests that the channel can close with Mg_i^{2+} blocking it. Based on these

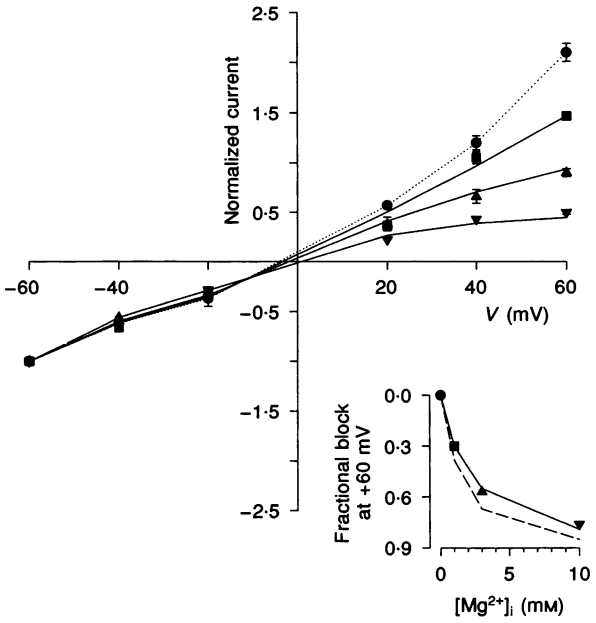

Figure 3. Voltage- and concentration-dependent inhibition by Mg_i^{2+} of mean patch current

The amplitude of mean patch current was normalized to that measured at −60 mV (see Methods). Symbols are experimental data. ●, control; ■, 1 mM Mg^{2+}; ▲, 3 mM Mg^{2+}; ▼, 10 mM Mg^{2+}. At positive potentials, each symbol represents the mean ± S.E.M. of at least three patches, except for 10 mM at +20 mV, which is the value of one patch. At negative potentials, each symbol represents the mean of two or three patches. S.E.M. values larger than the symbol size are shown. The fractional inhibition by Mg_i^{2+} at +60 mV (normalized current in the presence of Mg_i^{2+} divided by normalized current with 0 mM Mg_i^{2+}) is presented in the inset using the same symbols as in the main graph. The continuous line in the inset is the result of fitting eqn (3) to the plotted points. The dashed line represents the measured fractional inhibition of single-channel current using the data presented in Fig. 2*B* of Li-Smerin & Johnson (1996). The continuous lines in the main graph represent predicted normalized current, which was obtained by multiplying the plotted values of control (0 mM Mg_i^{2+}) normalized current by the value of eqn (3) (with K_{Rg} set to 1·4) at each voltage and Mg_i^{2+} concentration. Data points at 0 Mg_i^{2+} are connected with a dotted line.

results, we propose the following model to explain the effects of Mg_i^{2+} on both single-channel current and on channel gating:

$$\begin{array}{ccc} R + Mg^{2+} & \underset{\alpha}{\overset{\beta}{\rightleftharpoons}} & R^* + Mg^{2+} \\ & & k_- \Big\| k_+ \\ RMg^{2+} & \underset{\alpha_M}{\overset{\beta_M}{\rightleftharpoons}} & R^*Mg^{2+} \end{array}$$

Scheme 1

where R, R*, R^*Mg^{2+} and RMg^{2+} are the fully liganded receptors in the closed, open, open–blocked and closed–blocked states, respectively. α, α_M, β and β_M represent the indicated rate constants of channel gating. The values of the rate constants for block (k_+) and unblock (k_-) of Mg_i^{2+} were determined by Li-Smerin & Johnson (1996) based on a model that did not include either of the channel gating steps shown here. However, the approach that was used to measure k_+ and k_- should be valid regardless of how states R* and R^*Mg^{2+} can be exited, as long as only these states were occupied during bursts. Although Scheme 1 qualitatively explains our single-channel observations, the burst data are not sufficiently accurate to permit quantitative comparisons of the gating rate constants in the absence and presence of Mg_i^{2+}. Integration of Scheme 1 and our mean patch current data, which provided accurate measurements of inhibition over a wide range of Mg_i^{2+} concentrations and voltage, permits quantification of the effects of Mg_i^{2+} on channel gating.

Mean patch current should be proportional to the equilibrium occupancy of state R* in Scheme 1, which will depend on the equilibrium constants for each of the three transitions. The equilibrium constants will be defined as follows: K_D (equilibrium dissociation constant of Mg_i^{2+} for the open channel) $= k_-/k_+$; K_g (gating equilibrium constant of the unblocked channel) $= \alpha/\beta$; and K_{gM} (gating equilibrium constant of the blocked channel) $= \alpha_M/\beta_M$. Solution of Scheme 1 for equilibrium occupancy of R* in the presence and absence of Mg_i^{2+} results in the following equation:

$$I_{p,Mg}/I_{p,control} = 1/\{1 + ([Mg^{2+}]/(K_D K_{Rg}))\}, \quad (2)$$

where I_p is the mean patch current in the presence (Mg) and absence (control) of Mg_i^{2+}, $[Mg^{2+}]$ is the concentration of Mg_i^{2+}, and $K_{Rg} = (1 + K_g)/(1 + K_{gM})$. $I_{p,Mg}/I_{p,control}$ should be voltage dependent due to the voltage dependence of K_D, which can be described by the equation:

$$K_D = 8{\cdot}0 \exp(-V/36{\cdot}8),$$

where K_D is expressed in mM and V in mV (Johnson & Ascher, 1990; Li-Smerin & Johnson, 1996). This equation was used to replace K_D in eqn (2) to describe the

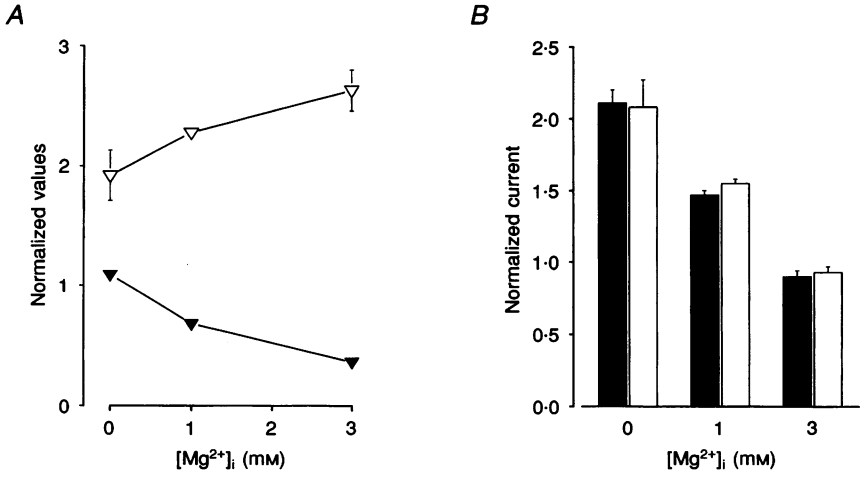

Figure 4. Comparison of measured mean patch current and predictions from single-channel analysis

At each Mg_i^{2+} concentration, each parameter value measured at +60 mV was normalized to the parameter value measured at −60 mV from the same patch. *A*, effects of Mg_i^{2+} on the product of the normalized burst frequency (f_b) and the burst duration (τ_b), and on the apparent single-channel current amplitude (i). ▽, $f_b\tau_b$; ▼, i. At each Mg_i^{2+} concentration, data for all the parameters were obtained from the same recordings ($n = 3$). Data for i are from Li-Smerin & Johnson (Fig. 2*B* in Li-Smerin & Johnson, 1996). The values of normalized f_b are shown in Fig. 1*A*. The values of normalized τ_b were: 1·24 ± 0·02, 1·16 ± 0·16 and 1·07 ± 0·16 for 0, 1 and 3 mM Mg_i^{2+}, respectively. Each symbol represents the mean ± S.E.M. (S.E.M. values smaller than the size of the symbol are not shown). *B*, comparison of the mean patch current measured directly (■) and the product of f_b, τ_b and i (□) calculated from the data shown in *A* (see text) at the indicated concentrations of Mg_i^{2+}. At each concentration of Mg_i^{2+}, the two sets of data were from the same three patches.

dependence on voltage and Mg_i^{2+} concentration of equilibrium current, assuming that K_g (see Nowak & Wright, 1992) and K_{gM} are much less voltage dependent than K_D. The resulting equation can be fitted to the data shown in the inset of Fig. 3 to find the value of K_{Rg}, which reflects the relationship of gating rate constants in the absence and presence of Mg_i^{2+}. These data points were chosen for fitting because they were measured at +60 mV, the voltage at which our measurements were most accurate. Since the data points shown in the inset of Fig. 3 were normalized to the value of mean patch current at −60 mV, the following normalized equation for fractional block was fitted to the data:

$$\frac{I_{p,n,Mg}}{I_{p,n,control}} = \frac{1 + [Mg^{2+}]/(40{\cdot}8K_{Rg})}{1 + [Mg^{2+}]/(8{\cdot}0\exp(-V/36{\cdot}8)K_{Rg})}, \quad (3)$$

where $I_{p,n}$ corresponds to I_p as defined for eqn (2) at voltage V (mV) normalized to the current measured at the same Mg_i^{2+} concentration at −60 mV. The best fit, performed with K_{Rg} as the only free parameter, was achieved with a value of K_{Rg} of 1·4. Equation (3) with K_{Rg} set equal to 1·4 was then used to predict the value of normalized patch current in the presence of Mg_i^{2+} at all voltages studied (Fig. 3). The close agreement between measured and predicted current further supports the hypothesis that inhibition of mean patch current is due to the combined effects of Mg_i^{2+} on single-channel current and channel gating by the mechanism described in Scheme 1.

The value of K_{Rg} is easier to interpret if values of K_g and K_{gM} are assumed to be much larger than 1. This would be true if the maximal value of the open probability of NMDA-activated channels (maximal P_o), which is equal to $\beta/(\beta + \alpha)$, is much less than 1. Estimates of maximal P_o have ranged from 0·04 to 0·3 (Jahr, 1992; Rosenmund, Clements & Westbrook, 1993; Hessler, Shirke & Malinow, 1993; Lin & Stevens, 1994; Rosenmund, Felts & Westbrook, 1995), corresponding to values of K_g of 23 to 2·3. The larger values of K_g may be more appropriate for whole-cell recordings (see, e.g. Huettner & Bean, 1988; Rosenmund *et al.* 1995). Since the data presented here also indicate that the value of K_{gM} is not much less than K_g, the approximation that K_g and K_{gM} are both much greater than 1 appears reasonable. In this case, $K_{Rg} \approx K_g/K_{gM}$. Because Mg_i^{2+} had no significant effect on burst duration (Fig. 1), α in Scheme 1 does not differ much from α_M, and K_g/K_{gM} should approximately equal β_M/β. Thus, we can estimate that $\beta_M/\beta = 1{\cdot}4$. The rate of channel opening is therefore approximately 1·4 times greater with Mg_i^{2+} blocking the channel than when the channel is unblocked, consistent with the results of burst analysis (Fig. 1*A*).

For simplicity, agonist binding steps are not shown in Scheme 1. Given the assumptions outlined, the same

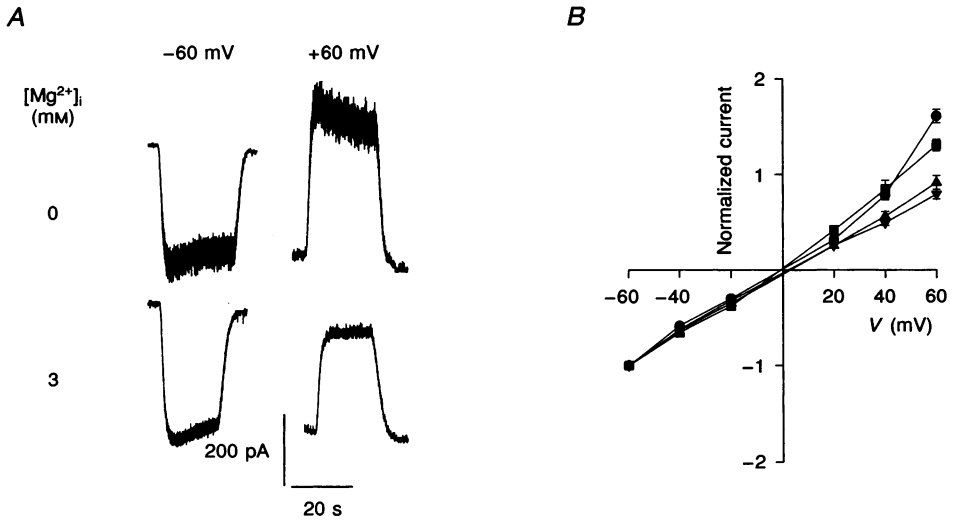

Figure 5. Voltage- and concentration-dependent inhibition by Mg_i^{2+} of NMDA-activated whole-cell currents

A, examples of whole-cell current records in 0 mM (upper panel) and 3 mM (lower panel) Mg_i^{2+} at −60 mV (left) and +60 mV (right). The two records at 0 Mg_i^{2+} were from the same cell, and the two records at 3 mM Mg_i^{2+} were from a second cell. All traces were filtered at 500 Hz. The ratio of the current at +60 mV to that at −60 mV is 1·53 and 1·0 for 0 and 3 mM Mg_i^{2+}, respectively. Data from these cells were included in *B*. *B*, *I–V* relationship of the whole-cell current in the absence (●) and presence of 1 mM (■), 3 mM (▲) and 10 mM (▼) Mg_i^{2+}. The amplitude of each current measurement was normalized to the amplitude measured at −60 mV in the same cell (see Methods). Each symbol represents the mean ± S.E.M. of experimental data from six cells for 0 and 10 mM Mg_i^{2+}, seven cells for 1 mM Mg_i^{2+}, and five cells for 3 mM Mg_i^{2+}. Data points were connected with straight lines.

conclusions can be drawn from a model that includes equilibrium of states RMg^{2+} and R with agonist-unbound states, providing that agonist affinity is the same whether or not Mg^{2+} is bound. Although the effect of Mg_i^{2+} on agonist affinity has not been examined, this seems a reasonable starting point for a model of the action of Mg_i^{2+}. Scheme 1 was also simplified by omission of a direct transition between states R and RMg^{2+}. It is not known at present whether the rate of this transition is significant. However, assuming that microreversibility is obeyed, the rates of this transition will have no effect on the equilibrium predictions made here.

Effect of Mg_i^{2+} on the whole-cell current

Measurements of inhibition by Mg_i^{2+} of steady-state whole-cell currents should, in principle, reproduce the results from mean patch current measurements. However, control of the intracellular environment and of membrane voltage are less complete during whole-cell experiments, and it is possible that NMDA receptor characteristics could depend on the patch-clamp configuration used (e.g. Sather, Johnson, Henderson & Ascher, 1990; Rosenmund *et al.* 1995). We therefore felt it was important to compare the effects of Mg_i^{2+} measured in whole-cell experiments with those measured in patches.

Inhibition by Mg_i^{2+} of the whole-cell current

Examples of the whole-cell current measured at −60 and +60 mV and in 0 and 3 mM Mg_i^{2+} are shown in Fig. 5*A*. The *I–V* relationship in the absence and the presence of Mg_i^{2+} is presented in Fig. 5*B*. Consistent with the results of mean patch current measurements, the NMDA-activated whole-cell current in the absence of Mg_i^{2+} exhibited a clear outward rectification. The normalized whole-cell current clearly decreased with increasing Mg_i^{2+} concentration at positive potentials but not obviously at negative potentials. At +60 mV and with 1, 3 and 10 mM Mg^{2+} in the pipette, the normalized current was reduced by 19, 43 and 50%, respectively, compared with the control values. These reductions at +60 mV were statistically significant (Kruskal–Wallis one-way analysis of variance followed by Mann–Whitney *U* test).

Comparison of the whole-cell current and the mean patch current

To determine whether the effects of Mg_i^{2+} on the NMDA-activated currents of patch and whole-cell recordings were equivalent, we compared normalized mean patch and whole-cell currents at +20, +40 and +60 mV (Fig. 6). There was qualitative agreement between the two preparations in that both normalized currents were reduced by Mg_i^{2+} in a voltage- and concentration-dependent manner. However, the normalized whole-cell current was generally smaller than normalized mean patch current at 0 and 1 mM Mg_i^{2+}, but was larger at 10 mM Mg_i^{2+}. At 3 mM Mg_i^{2+}, the two normalized currents were nearly equal.

Two intriguing points emerge from the comparison in Fig. 6: normalized patch and whole-cell currents in 0 mM Mg_i^{2+} differ, and the inhibition of mean patch current depends on Mg_i^{2+} concentration more strongly than the inhibition of whole-cell current, especially at +60 mV. A

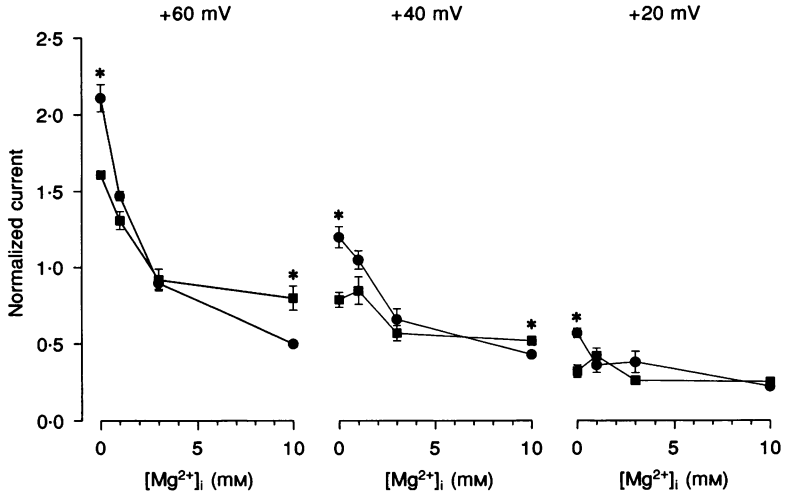

Figure 6. Comparison of normalized whole-cell and mean patch currents in the absence and presence of Mg_i^{2+}

The mean patch data (●) are replotted from Fig. 4 and the whole-cell data (■) are replotted from Fig. 5. Currents measured at +60 mV (left), +40 mV (middle) and +20 mV (right) were normalized to those measured at −60 mV from the same cell or patch. Symbols, representing the means ± S.E.M. of the experimental data, were connected with straight lines. Statistically significant differences between the normalized mean patch and the whole-cell currents are indicated by asterisks ($P < 0{\cdot}05$; two-tailed *t* test).

plausible explanation for both of the differences is that, during whole-cell recording, the free Mg^{2+} concentration in the neuron was regulated such that it was different from the pipette Mg^{2+} concentration. We first tested the hypothesis that the values of the two normalized currents in 0 mM Mg_i^{2+} were different due to block of whole-cell current by residual Mg^{2+} in the cell under study.

Effect of Mg_i^{2+} chelators on the whole-cell current at 0 mM Mg_i^{2+}

The normalized whole-cell current would be smaller than the normalized mean patch current at 0 mM Mg_i^{2+} if residual Mg_i^{2+} (Mg^{2+} that remained free inside cells despite dialysis with 0 Mg_i^{2+} solution) partially blocked whole-cell current. We tested this hypothesis by comparing the whole-cell currents of cells dialysed with three different 0 Mg_i^{2+} solutions: one with no Mg^{2+} chelators (no EGTA, EDTA or Na_2-ATP), one with EDTA alone to chelate Mg_i^{2+}, and one with EDTA plus Na_2-ATP to chelate Mg_i^{2+}. Our use of Na_2-ATP along with EDTA in some experiments was based on the observation that EDTA plus Na_2-ATP chelated residual Mg_i^{2+} more effectively than EDTA alone in PC12 cells (Sands & Barish, 1992). If residual Mg_i^{2+} inhibited whole-cell current, then inclusion of Mg^{2+} chelators in the pipette solution should increase the whole-cell current at positive potentials. As shown in Fig. 7*A*, there was no consistent change in the normalized whole-cell current at +60 mV with time for any group. The means of measurements at all time points for each of the three groups (Fig. 7*B*) showed no significant difference between the 'no chelators' and either of the Mg^{2+}-chelator groups. These results suggest that the difference between the normalized whole-cell and mean patch currents at 0 mM Mg_i^{2+} was not due to block by residual Mg_i^{2+}.

Effect of EGTA on the Mg_i^{2+} inhibition of the whole-cell current

We next investigated the observation that whole-cell current appeared less sensitive to inhibition by Mg_i^{2+} than did mean patch current (Fig. 6). One possible explanation for this difference is that free Mg^{2+} within clamped neurons was maintained at a lower concentration than the free Mg^{2+} in the pipette solution. To test this hypothesis, we determined whether the EGTA and EGTA–Mg_i^{2+} typically included in the pipette solution (see Li-Smerin & Johnson, 1996) acted to enhance the block by Mg_i^{2+} of whole-cell current. Since EGTA has an apparent equilibrium dissociation constant for Mg^{2+} of about 10 mM under the conditions used here, inclusion of 10 mM EGTA should have helped buffer the free Mg^{2+} concentration in the cell close to the free concentration in the pipette. If this buffering action of EGTA partially counteracted any cellular processes that tended to lower Mg_i^{2+} concentration, then use of the EGTA-containing pipette solution would

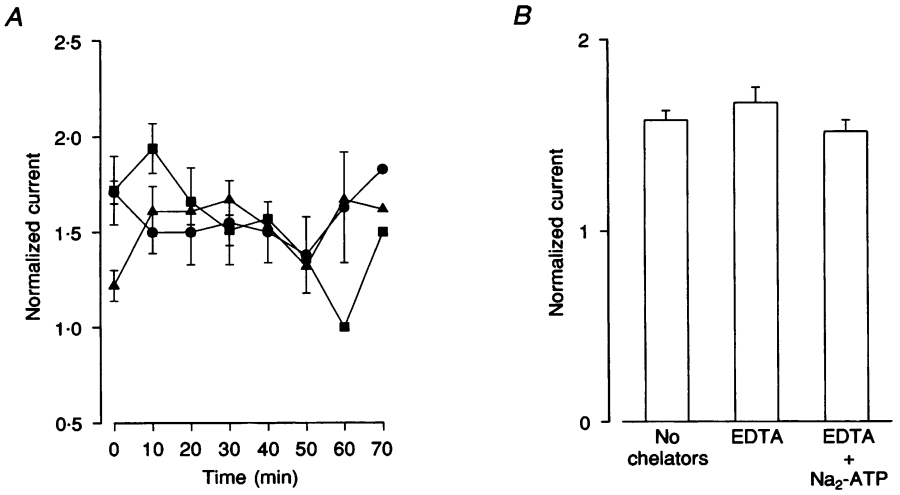

Figure 7. Effect of inclusion of Mg_i^{2+} chelators in the pipette solution on normalized NMDA-activated whole-cell current at +60 mV

For this set of experiments, the NMDA-activated current was measured only at −60 and +60 mV. Measurements at −60 mV were made immediately before and after each measurement at +60 mV. The preceding measurement at −60 mV was used to normalize the measurements at +60 mV and the subsequent measurement at −60 mV was used to judge the validity of data (see Methods). *A*, time course of the normalized whole-cell current measured in the absence and presence of Mg_i^{2+} chelators. Symbols represent the mean ± S.E.M. of the experimental data. ●, no chelators; ■, EDTA; ▲, EDTA + Na_2-ATP. Data are from three to six cells for the points with error bars and two or one cells for the points without error bars. The no chelators group contained no EDTA, Na_2-ATP or EGTA. The values at 0 min represent the first measurements of whole-cell currents, typically at about 5 min after initiating whole-cell recording. The data points were connected with straight lines. *B*, means (± S.E.M.) of all the measurements for each group in *A*. There was no significant difference between groups (ANOVA).

have enhanced the observed inhibition of whole-cell current.

We compared the normalized whole-cell current at +60 mV in the absence and presence of EGTA. The values of the normalized whole-cell currents at +60 mV with no EGTA in the pipette solution were 1·68 ± 0·05 ($n = 9$), 1·86 ± 0·3 ($n = 3$) and 1·04 ± 0·20 ($n = 3$) for 0, 1 and 10 mM free pipette Mg^{2+}, respectively. The values with EGTA included in the pipette solution were 1·61 ± 0·01 ($n = 6$), 1·31 ± 0·06 ($n = 7$) and 0·80 ± 0·08 ($n = 6$) for 0, 1 and 10 mM free pipette Mg^{2+}, respectively. The inhibition was significant at both 1 and 10 mM Mg_i^{2+} in the presence of EGTA, but only at 10 mM Mg_i^{2+} in its absence (ANOVA followed by Tukey's HSD test). These results are consistent with the hypothesis that, during whole-cell recording, a cell can maintain the Mg_i^{2+} concentration below the pipette concentration.

The NMDA-activated whole-cell current has been reported to be inactivated by Ca^{2+}, predominantly at negative potentials (Legendre, Rosenmund & Westbrook, 1993). Since we measured the steady-state whole-cell current and normalized it to that at −60 mV, we were concerned that prevention of the Ca^{2+}-dependent inactivation of whole-cell current by EGTA or EDTA may have been a confounding factor in the interpretation of our results. However, our observation that the normalized whole-cell current at 0 mM Mg_i^{2+} without EGTA (1·7) was not significantly different from that with EGTA (1·6) or with EDTA (1·7; Fig. 7) suggests that Ca^{2+}-dependent inactivation did not confound the interpretation of our results.

Time dependence of block by Mg_i^{2+} of whole-cell current

It is also possible that differences in the characteristics of the NMDA receptor in the whole-cell and patch configurations caused the difference in the sensitivities to inhibition by Mg_i^{2+}. If this were the case, the degree of inhibition by Mg_i^{2+} of normalized whole-cell current could be expected to change with time of dialysis (see, e.g. Sather, Dieudonné, MacDonald & Ascher, 1992; Rosemund *et al.* 1995). We examined this possibility by comparing normalized whole-cell current at +60 mV in the presence of Mg_i^{2+} (with 10 mM EGTA) about 5 min after initiating whole-cell recording ('early'; the conditions used for Figs 5 and 6) with the response 30 min later ('late'). The values of normalized whole-cell current were: 0·92 ± 0·11 (early) and 0·90 ± 0·11 (late) for 3 mM Mg_i^{2+}; and 0·70 ± 0·02 (early) and 0·82 ± 0·15 (late) for 10 mM Mg_i^{2+} ($n = 3$ in all cases). Neither of the differences between the early and late normalized currents was significant, suggesting that the effects of Mg_i^{2+} on whole-cell currents are rapid and stable.

Effects of Na^+–Mg^{2+} exchange on the Mg_i^{2+} inhibition of whole-cell current

One of the mechanisms that normally regulates the free Mg_i^{2+} concentration in numerous types of mammalian cells is Na^+–Mg^{2+} exchange (see, e.g. Flatman, 1991; Murphy, Freudenrich & Lieberman, 1991). We explored the possibility that Na^+–Mg^{2+} exchange helped maintain the free Mg_i^{2+} concentration below the concentration in the pipette solution, and thereby limited the inhibition of whole-cell current. We reduced the Na^+ gradient across the membrane by first increasing the pipette Na^+ concentration from 0 to 65 mM (and decreasing the Cs^+ concentration by 65 mM). The normalized whole-cell current at +60 mV with 10 mM free Mg^{2+} and 10 mM EGTA in the pipette was 0·97 ± 0·07 ($n = 3$). We then lowered the extracellular Na^+ concentration to 65 mM (and increased the Cs^+ concentration from 0 to 75 mM) in the same experiments. The normalized whole-cell current was 0·96 ± 0·02. Neither of these values was significantly different from 0·80 ± 0·08 ($n = 6$), the value of the normalized current measured with an identical concentration of free Mg_i^{2+} and EGTA in the control (0 Na^+) pipette solution and with the control (140 mM Na^+) extracellular solution. These results do not support the hypothesis that Na^+–Mg^{2+} exchange played a role in the regulation of Mg_i^{2+} concentration during our whole-cell experiments.

DISCUSSION

Effect of Mg_i^{2+} on channel gating

Effect of Mg_i^{2+} on bursts

To explain the voltage- and concentration-dependent block by Mg_i^{2+} of single-channel NMDA-activated current, a two-state model, $R^* + Mg^{2+} \rightleftharpoons R^*Mg^{2+}$, was previously adopted (Johnson & Ascher, 1990; Li-Smerin & Johnson, 1996). This model of open-channel block cannot be used to investigate the interaction of Mg_i^{2+} with channel gating because it lacks channel transition steps. To interpret the results of burst analysis, we needed to extend this model to include gating steps. The 'sequential' scheme (Neher & Steinbach, 1978), which includes gating steps, postulates that the channel cannot return to the closed state while it is blocked; as a result, the burst duration is predicted to increase with increasing concentration of blocker. Assuming the channel is predominantly in the open state during bursts (see below), the mean burst duration that should be observed if Mg_i^{2+} were a sequential blocker can be predicted (Neher & Steinbach, 1978). Using the value of K_D (mM) calculated from the equation $K_D = 8{\cdot}0\exp(-V/36{\cdot}8)$ (V in mV), the predicted mean burst durations at +60 mV would be 18·7 and 33·2 ms in the presence of 1 and 3 mM Mg_i^{2+}, respectively. These values are 1·7 and 3·2 times the corresponding observed values (Fig. 1*B*), indicating that the simple sequential scheme does not correctly describe the effect of Mg_i^{2+} binding on channel gating.

One possible explanation is that there is a second, slow inhibitory action of Mg_i^{2+} that can terminate bursts. The observation that the burst frequency was increased significantly in the presence of Mg_i^{2+} (Fig. 1*A*), however,

argues against this possibility. The explanation that we prefer is that bursts can be terminated by closure of an open NMDA-activated channel while it is blocked by Mg_i^{2+}, as shown by Scheme 1. The increase in burst frequency induced by Mg_i^{2+} suggests that the opening rate of Mg_i^{2+}-blocked closed channels is greater than the opening rate of unblocked closed channels. A related model in which the NMDA-activated channel can close while blocked by Mg_o^{2+} has been proposed by Jahr & Stevens (1990) to explain the effects of Mg_o^{2+} on bursts. However, in their analysis the rate of closure of the NMDA-activated channel was estimated to be decreased by a factor of 1·3 when Mg_o^{2+} occupied the channel, whereas we found that the rate of closure was not significantly altered by Mg_i^{2+} binding.

In performing burst analysis we ignored closures of $\leqslant 1$ ms and openings of $\leqslant 0{\cdot}4$ ms in both control and experimental recordings to overcome the problem of frequent noise-induced threshold crossings due to Mg_i^{2+} action. We thereby ignored the great majority of noise-induced threshold crossings, but we also counted as within burst some brief closures not due to block by Mg_i^{2+} (see, e.g. Gibb & Colquhoun, 1992). This could have made burst duration relatively insensitive to the route(s) by which state R^*Mg^{2+} can be exited if the channel had spent a large fraction of the burst in a closed state. However, measurement of channel open probability during bursts indicates that the channel is closed for only a small fraction of the burst duration (S. Antonov & J. W. Johnson, unpublished observations; see also Gibb & Colquhoun, 1992). Thus, burst duration should have changed in proportion to the duration per opening of states $R^* + R^*Mg^{2+}$, as desired in burst analysis of blocker action. The limited range of conditions under which bursts could be analysed and the need to eliminate numerous brief events nevertheless led us to test the validity of our conclusions using a different approach.

Effect of Mg_i^{2+} on mean patch current and integration with burst data

Inhibition by Mg_i^{2+} of mean patch current resembled inhibition by Mg_i^{2+} of apparent single-channel current in that both are voltage and Mg_i^{2+} concentration dependent. However, fractional mean patch currents in the presence of Mg_i^{2+} were larger than fractional apparent single-channel currents. This difference is consistent with the increase in burst frequency observed in the presence of Mg_i^{2+}, which should have partially compensated for the reduction in apparent single-channel current. Mean patch current measurements are in quantitative agreement with predictions based on the effects of Mg_i^{2+} on burst parameters and apparent single-channel current, corroborating the burst analysis. An equation based on Scheme 1 well fitted the voltage and Mg_i^{2+} concentration dependence of mean patch current, further supporting the idea that Mg_i^{2+}-blocked channels can close. Using the results of curve fitting, we can estimate at any voltage the value of the apparent inhibition constant that characterizes the effect of Mg_i^{2+} on mean patch current ($K_{I,app}$). From eqn (2), $K_{I,app}$ equals $K_D K_{Rg}$. Thus,

$$K_{I,app} = 11{\cdot}3\exp(-V/36{\cdot}8), \quad (4)$$

where $K_{I,app}$ is expressed in mM and V is in mV.

Our results suggest that the closing rates of Mg_i^{2+}-blocked channels and unblocked channels are similar, while the opening rate of Mg_i^{2+}-blocked channels is about 1·4 times greater than the opening rate of unblocked channels. Thus, when Mg_i^{2+} is bound in the channel, the closed state of the channel is destabilized. Modification of channel gating appears to be a common consequence of channel occupancy by either blocking (e.g. Armstrong, 1971) or permeant (e.g. Ascher, Marty & Neild, 1978) ions. It was possible to quantify the factor by which the closed state of the high-conductance K^+ channel is destabilized during block by Ba^{2+} (Miller, Latorre & Reisin, 1987) or Cs^+ (Demo & Yellen, 1992). Through different mechanisms (Neyton & Pelleschi, 1991; Demo & Yellen, 1992), block by either ion results in destabilization of the closed state by about a factor of 10. The effect of Mg_i^{2+} on the closed state of the NMDA-activated channel is weak by comparison.

Comparison of mean patch current and whole-cell current

The voltage and concentration dependence of the block by Mg_i^{2+} of whole-cell NMDA-activated currents suggests that the mechanism of block is qualitatively similar at the patch and whole-cell levels. However, both in the absence and presence of Mg_i^{2+}, we observed quantitative differences between normalized measurements of mean patch and whole-cell currents. We will discuss three possible explanations for these differences.

Regulation of free Mg_i^{2+} concentration

Many types of mammalian cells have an enormous capacity for regulating free Mg_i^{2+} concentration, which is typically only 5–10% of the total intracellular Mg^{2+} concentration (for reviews see Flatman, 1991; Murphy *et al.* 1991; Romani & Scarpa, 1992). We investigated two ways in which any intracellular regulatory mechanisms that remained intact during whole-cell dialysis could have interfered with our ability to control Mg_i^{2+} concentration. First, Mg^{2+} may have been released from intracellular stores during dialysis with 0 Mg^{2+} solutions, resulting in block of whole-cell current by residual Mg_i^{2+}. This possibility was suggested by the observation that normalized whole-cell current was smaller than normalized mean patch current at positive potentials with a 0 Mg^{2+} pipette solution (see also Nowak & Wright, 1992). We tested this possibility by repeating our whole-cell measurements using 0 Mg^{2+} pipette solutions that contained the Mg^{2+} chelators EDTA or EDTA plus Na_2-

ATP. This procedure was based on the observation of Sands & Barish (1992) that relief of block by residual Mg_i^{2+} of neuronal nicotinic ACh (nACh)-activated currents of PC12 cells required use of both of these Mg^{2+} buffers. Our results, however, suggest that residual Mg_i^{2+} did not cause a significant block of whole-cell currents activated by NMDA. The difference between our conclusions and those of Sands & Barish (1992) may result from the greater affinity of Mg_i^{2+} for block of the neuronal nACh receptor of PC12 cells than for block of the NMDA receptor. At present we do not have an explanation for the discrepancy between the normalized mean patch and whole-cell currents measured with 0 Mg^{2+} pipette solution.

The second way in which mechanisms that regulate intracellular Mg^{2+} may have influenced our experiments is by maintaining the intracellular Mg^{2+} concentration below the pipette concentration when Mg^{2+} was included in the pipette solution. We tested this possibility by examining the effects of an EGTA–Mg^{2+} intracellular solution. The affinity of EGTA for Mg^{2+} permits it to buffer Mg^{2+} concentration in the millimolar range. We found that the EGTA–Mg^{2+} solutions enhanced the inhibition at positive potentials of whole-cell currents, supporting the idea that mechanisms that reduce intracellular Mg^{2+} were active in our whole-cell experiments.

Brocard, Rajdev & Reynolds (1993) reported that Na^+–Mg^{2+} exchange is active in cultured neurons. Our results did not support the idea that Na^+–Mg^{2+} exchange played a role under our experimental conditions. However, since the net gradient for Na^+–Mg^{2+} exchange in all our experiments was outward (since we used 0 mM Mg_o^{2+}), we cannot completely exclude a contribution from Na^+–Mg^{2+} exchange.

Characteristics of the channel

A difference in the characteristics of NMDA-activated channels in whole cells *versus* outside-out patches could also explain the difference between the two preparations in their sensitivities to pipette Mg^{2+} concentration. An example of an NMDA-receptor property that differs between whole-cell and patch configurations is glycine-insensitive desensitization. Both the speed and amplitude of glycine-insensitive desensitization are greater in outside-out or nucleated patches than in whole-cell recordings (Sather *et al.* 1990, 1992). As the time during whole-cell recording progressed, the speed and amplitude of desensitization of whole-cell responses approached those of patch responses (Benveniste, Clements, Vyklický & Mayer, 1990; Vorobjev & Sharonova, 1994). We did not observe such an evolution of Mg_i^{2+} block of whole-cell current during a 30 min recording period. However, washout in whole-cell recordings (loss of intracellular constituents due to exchange with the pipette solution) is highly variable with time and experimental conditions. We therefore cannot exclude the possibility that apparently different inhibition by Mg_i^{2+} of whole-cell and patch currents may be due to differences between these two configurations in channel properties.

Adequacy of voltage clamp

A third possible cause of the difference between the Mg^{2+} dependence of current inhibition in patch and whole-cell experiments is insufficient voltage control in our whole-cell recordings. Insufficient voltage control, resulting from access resistance errors and/or space-clamp problems, would have decreased the apparent effectiveness of Mg_i^{2+} block at dendritic receptors because of the voltage dependence of Mg_i^{2+} action. The magnitude of voltage errors due to either problem would have been exacerbated by larger membrane currents. If inadequate voltage control affected the values of normalized current measured in whole-cell experiments, then there should have been a negative correlation between current amplitude at +60 mV and normalized inhibition by Mg_i^{2+} at +60 mV. However, we found no significant correlation between the normalized current at +60 mV and current amplitude in any of our experimental groups (Pearson correlation test). In addition, excluding from analysis all cells with maximum currents larger than 1 nA (about 25% of all experiments) did not significantly change the averaged current ratio for any group.

In conclusion, the data presented here favour the idea that processes that regulate Mg_i^{2+} concentration in intact neurons remain active during whole-cell experiments. However, further experimentation will be required to determine conclusively the explanation for the apparent difference between the inhibition by Mg_i^{2+} of whole-cell and patch currents. This difference warrants caution in estimating from whole-cell data the magnitude of NMDA-activated current inhibition by Mg_i^{2+}.

Functional implication of Mg_i^{2+} block

Both our mean patch current and whole-cell data support the previous conclusion (Johnson & Ascher, 1990) that blockade of the NMDA response by Mg_i^{2+} is unlikely to be significant at physiological Mg_i^{2+} concentrations, except during actions potentials. However, inhibition by higher Mg_i^{2+} concentrations can be significant under pathophysiological conditions. Brocard *et al.* (1993) have shown that extracellular glutamate can increase the Mg_i^{2+} concentration to over 10 mM through a NMDA receptor-mediated mechanism. Our mean patch currents results (eqn (4)) indicate that the apparent dissociation constant of Mg_i^{2+} at 0 mV is 11·3 mM. Thus, under ischaemic conditions, when membrane potential approaches 0 mV and extracellular glutamate concentration increases, the block by Mg_i^{2+} of the NMDA response could be significant. As a result, the influx of Ca^{2+} and Na^+ into cells could be attenuated and cell damage diminished.

ARMSTRONG, C. M. (1971). Interaction of tetraethylammonium ion derivatives with the potassium channels of giant axons. *Journal of General Physiology* **58**, 413–437.

ASCHER, P., MARTY, A. & NEILD, T. O. (1978). Life time and elementary conductance of the channels mediating the excitatory effects of acetylcholine in *Aplysia* neurons. *Journal of Physiology* **278**, 177–206.

ASCHER, P. & NOWAK. L. (1988). The role of divalent cations in the *N*-methyl-D-aspartate responses of mouse central neurones in culture. *Journal of Physiology* **399**, 247–266.

BENVENISTE, M., CLEMENTS, J., VYKLICKÝ, L. JR & MAYER, M. L. (1990). A kinetic analysis of the modulation of *N*-methyl-D-aspartic acid receptors by glycine in mouse cultured hippocampal neurones. *Journal of Physiology* **428**, 333–357.

BROCARD, J. B., RAJDEV, S. & REYNOLDS, I. J. (1993). Glutamate-induced increases in intracellular free Mg^{2+} in cultured cortical neurons. *Neuron* **11**, 1–20.

COCHRAN, W. G. (1956). *Statistical Methods.* Iowa State University Press, Ames, IA, USA.

COLQUHOUN, D. & SIGWORTH. F. J. (1983). Fitting and statistical analysis of single-channel records. In *Single-Channel Recording*, ed. SAKMANN, B. & NEHER, E., pp. 191–263. Plenum Press, New York.

DEMO, S. D. & YELLEN, G. (1992). Ion effects on gating of the Ca^{2+}-activated K^+ channel correlate with occupancy of the pore. *Biophysical Journal* **61**, 639–648.

FLATMAN, P. W. (1991). Mechanisms of magnesium transport. *Annual Review of Physiology* **53**, 259–271.

GIBB, A. J. & COLQUHOUN, D. (1992). Activation of *N*-methyl-D-aspartate receptors by L-glutamate in cells dissociated from adult rat hippocampus. *Journal of Physiology* **456**, 143–179.

HAMILL, O. P., MARTY, A., NEHER, E., SAKMANN, B. & SIGWORTH, F. J. (1981). Improved patch-clamp techniques for high resolution current recording from cells and cell-free membrane patches. *Pflügers Archiv* **391**, 85–100.

HESSLER, N. A., SHIRKE, A. M. & MALINOW, R. (1993). The probability of transmitter release at a mammalian central synapse. *Nature* **366**, 569–572.

HUETTNER, J. E. & BEAN, B. P. (1988). Block of *N*-methyl-D-aspartate-activated current by the anticonvulsant MK-801: Selective binding to open channels. *Proceedings of the National Academy of Sciences of the USA* **85**, 1307–1311.

JAHR, C. E. (1992). High probability opening of NMDA receptor channels by L-glutamate. *Science* **255**, 470–472.

JAHR, C. E. & STEVENS, C. F. (1990). A quantitative description of NMDA receptor-channel kinetic behavior. *Journal of Neuroscience* **10**, 1830–1837.

JOHNSON, J. W. & ASCHER, P. (1990). Voltage-dependent block by intracellular Mg^{2+} of *N*-methyl-D-aspartate-activated channels. *Biophysical Journal* **57**, 1085–1090.

LEGENDRE, P., ROSENMUND, C. & WESTBROOK, G. L. (1993). Inactivation of NMDA channels in cultured hippocampal neurons by intracellular calcium. *Journal of Neuroscience* **13**, 674–684.

LI, Y.-Y. & JOHNSON, J. W. (1992). Differential block by intracellular Mg^{2+} of the NMDA response in whole-cell and outside-out patch recordings. *Society for Neuroscience Abstracts* **18**, 652.

LIN, F. & STEVENS, C. F. (1994). Both open and closed NMDA receptor channels desensitize. *Journal of Neuroscience* **14**, 2153–2160.

LI-SMERIN, Y. & JOHNSON, J. W. (1994). Effect of intracellular Mg^{2+} buffering on the block of NMDA responses in cultured neurons. *Society for Neuroscience Abstracts* **20**, 236.

LI-SMERIN, Y. & JOHNSON, J. W. (1996). Kinetics of the block by intracellular Mg^{2+} of the NMDA-activated channel in cultured rat neurons. *Journal of Physiology* **491**, 121–135.

MILLER, C., LATORRE, R. & REISIN, I. (1987). Coupling of voltage-dependent gating and Ba^{2+} block in the high-conductance, Ca^{2+}-activated K^+ channel. *Journal of General Physiology* **90**, 427–449.

MURPHY, E., FREUDENRICH, C. C. & LIEBERMAN, M. (1991). Cellular magnesium and Na/Mg exchange in heart cells. *Annual Review of Physiology* **53**, 273–287.

NEHER, E. & STEINBACH, J. H. (1978). Local anaesthetics transiently block currents through single acetylcholine-receptor channels. *Journal of Physiology* **277**, 153–176.

NEYTON, J. & PELLESCHI, M. (1991). Multi-ion occupancy alters gating in high-conductance, Ca^{2+}- activated K^+ channels. *Journal of General Physiology* **97**, 614–665.

NOWAK, L. M. & WRIGHT, J. M. (1992). Slow voltage-dependent changes in channel open-state probability underlie hysteresis of NMDA responses in Mg^{2+}-free solution. *Neuron* **8**, 181–187.

PUSCH, M. & NEHER, E. (1988). Rates of diffusional exchange between small cells and a measuring patch pipette. *Pflügers Archiv* **411**, 204–211.

ROMANI, A. & SCARPA, A. (1992). Regulation of cell magnesium. *Archives of Biochemistry and Biophysics* **298**, 1–12.

ROSENMUND, C., CLEMENTS, J. D. & WESTBROOK, G. L. (1993). Nonuniform probability of glutamate release at a hippocampal synapse. *Science* **262**, 754–757.

ROSENMUND, C., FELTS, A. & WESTBROOK, G. L. (1995). Synaptic NMDA receptor channels have a low open probability. *Journal of Neuroscience* **15**, 2788–2795.

SANDS, S. B. & BARISH, M. E. (1992). Neuronal nicotinic acetylcholine receptor currents in phaeochromocytoma (PC12) cells: dual mechanisms of rectification. *Journal of Physiology* **447**, 467–487.

SATHER, W., DIEUDONNÉ, S., MACDONALD, J. & ASCHER, P. (1992). Activation and desensitization of *N*-methyl-D-aspartate receptors in nucleated outside-out patches from mouse neurones. *Journal of Physiology* **450**, 643–672.

SATHER, W., JOHNSON, J. W., HENDERSON, G. & ASCHER, P. (1990). Glycine-insensitive desensitization of NMDA responses in cultured mouse embryonic neurons. *Neuron* **4**, 725–731.

VANDENBERG, C. A. (1987). Inward rectification of a potassium channel in cardiac ventricular cells depends on internal magnesium ions. *Proceedings of the National Academy of Sciences of the USA* **84**, 2560–2564.

VOROBJEV, V. S. & SHARONOVA, I. N. (1994). Tetrahydroaminoacridine blocks and prolongs NMDA receptor-mediated responses in a voltage-dependent manner. *European Journal of Pharmacology* **253**, 1–8.

ZAREI, M. M. & DANI, J. A. (1995). Structural basis for explaining open-channel blockade of the NMDA receptor. *Journal of Neuroscience* **15**, 1446–1454.

Acknowledgements

We thank Dr Philippe Ascher and James Dilmore for their helpful criticism of the manuscript, Dr Jerry Wright for providing software for the analysis of single-channel data, and Mr Keith Newell for skilful technical assistance. This work was supported by National Institutes of Health Grants MH 45817 and MH 00944.

Received 15 November 1994; accepted 23 August 1995.